Sustainable Materials and Technologies 39 (2024) e00859

Contents lists available at ScienceDirect

Sustainable Materials and Technologies

journal homepage: www.elsevier.com/locate/susmat

Effects of using tea waste as an additive in the production of solid bricks in terms of their porosity, thermal conductivity, strength and durability

Laura Crespo-López [a,*], Chiara Coletti [b], Anna Arizzi [a], Giuseppe Cultrone [a]

[a] Department of Mineralogy and Petrology, Faculty of Sciences, University of Granada, Avda. Fuentenueva s/n, 18002 Granada, Spain
[b] Department of Geosciences, Università Degli Studi Di Padova, Via Giovanni Gradenigo, 6, 35131 Padova, Italy

ARTICLE INFO

Keywords:
Bricks
Tea waste
Recycling
Thermal conductivity
Innovation

ABSTRACT

In this paper, we investigated the use of tea waste as an additive in the production of traditional bricks. This could provide several environmental and economic benefits, as well as improving thermal insulation in construction. To this end, we produced brick samples with 0, 5 and 10 w% of tea waste mixed with a clayey material from Teruel (Spain) that was rich in quartz and phyllosilicates and had smaller amounts of carbonates. These samples were fired at 800, 950 and 1100 °C in an electric oven. We then analysed and discussed their chemical, mineralogical, textural and physical-mechanical behaviour and evaluated their durability in response to salt crystallization. The pore system of the bricks was examined using a combination of different analytical techniques (hydric tests, mercury intrusion porosimetry and digital image analysis). We also evaluated their thermal conductivity and observed that an increase in the firing temperature and the amount of tea waste altered the texture of the bricks, increasing their porosity. This happened above all at 1100 °C, where it led to the appearance of a new family of pores and increased the porosity to about 39% for bricks made with 10 w% added tea waste. The increased porosity made the bricks lighter. The bricks made with tea waste showed higher levels of water absorption and poorer mechanical strength. Our results suggest that the addition of tea residues strongly decreases the thermal conductivity and heat diffusion capacity of the bricks. They could therefore be used as lightweight bricks for the thermal insulation of buildings.

1. Introduction

Tea is one of the oldest traditional beverages in the world and one of the most widely consumed non-alcoholic drinks after coffee, with consumption estimated at 85 l per person per year. Tea is particularly important in Asia, Eastern Europe, and the UK [1]. There are records of its consumption as early as 1500 BCE in the Yunnan province of China [2], where it first appeared as a medicinal drink due to the antioxidant, diuretic and anti-inflammatory properties of *Camellia Sinesis* [3,4] the plant commonly known as tea. The particular variety of tea produced varied greatly depending on the harvesting process and the treatment applied to it [5,6]. However, it was not until the 16th century that its consumption became popular in the West, where it became the emblematic hot drink in the United Kingdom [7,8]. In the early 20th century, the sale of tea became even more popular worldwide due to the invention of the tea bag [9]. In 2020, a total of just over seven million tonnes of tea were produced worldwide. Asia accounted for around 83% of this volume, growing and harvesting around 5.8 million tonnes [10]. The tea industry is on the rise, and is expected to grow by 4.22% per year between 2023 and 2025 (https://statista.com). In line with the increase in tea consumption, the amount of waste is growing rapidly, resulting in a substantial loss of biomass and increasing environmental stress. Tea residues, also known as tea waste or tea grounds, are known to be rich in certain organic compounds, in particular lignin and holocellulose [11,12]. These compounds play a crucial role in the formation of porous structures in construction materials. During the tea-leaf manufacturing process, these components become interwoven within the plant's cell walls. Later, when the tea is brewed, they are released into the liquid phase, and after the tea is consumed, some remain behind in the residues [13]. Hussain et al. [14] and Li et al. [15] have postulated that tea residues could be used to produce biochar, which in turn could be used as a nitrogen-rich biomass precursor for preparing pollutant adsorbents. Research into the possible reuse of tea waste biomass in practical applications has so far centred on converting it into bioadsorbents [16], agricultural compost [17,18] or animal feed [19,20], although more research is required in this field and other alternatives must be proposed.

* Corresponding author.
E-mail addresses: lcrespo@ugr.es (L. Crespo-López), chiara.coletti@unipd.it (C. Coletti), arizzina@ugr.es (A. Arizzi), cultrone@ugr.es (G. Cultrone).

https://doi.org/10.1016/j.susmat.2024.e00859
Received 29 November 2023; Received in revised form 16 January 2024; Accepted 4 February 2024
Available online 10 February 2024

For its part, clay is now considered an exhaustible resource, to such an extent that in some countries, such as Australia or China, its use in the manufacture of bricks has been restricted and the use of alternative waste or recycled materials is being actively promoted [21–23]. To this end, research has been conducted into the use of various organic additives in bricks [24–26]. Results have demonstrated their effectiveness as pore agents/developers, and the improvements they can bring in terms of insulation and the reduction of heat transmission [25]. The resulting bricks have also been shown to be well suited for use as lightweight building materials [26]. With this in mind, in this paper, we explore the possible use of tea residues (5 and 10 w %) as additives in the production of traditional handmade bricks. There are various reasons for research on this subject. Firstly, the use of additives reduces the depletion of natural supplies of clay, the main raw material used in brickmaking. Secondly, the reuse of the waste generated by tea-drinking in the brick manufacturing process can produce energy savings compared to conventional brickmaking. This is due to the biomass capacity of the additive, which produces additional heat during firing. Thirdly, the addition of tea waste enables the production of lightweight bricks with optimal thermal insulation properties that can help reduce domestic winter heating bills.

Although various research studies have already been conducted into the use of tea waste as an additive in brick manufacture, we believe that there are still many important gaps that our research seeks to fill. To this end we focus on various issues that we consider essential for appraising the technical quality of the bricks. These include: 1) measuring the colour of the fired bricks and assessing how the addition of tea waste influences the colour values. Colour is of great importance in the field of architectural heritage, in that it is one of the key factors in the choice of a replacement brick when restoring the façade of a historic building; 2) the need to determine the compactness of bricks and relate it to their compressive strength. In this research, we combine the measurement of compressive strength with that of ultrasound velocity so as to provide a more complete picture of the performance of the bricks from a petrophysical point of view; 3) the study of the porous system and pore size distribution and how they are altered by the addition of the tea waste.

Previous research on this issue has thrown up interesting results albeit with certain important differences compared to our research, which we will now go on to explain. Hamilton and Hall [27] considered that further studies were needed to understand the effect of added tea residue on the compressive strength and thermal conductivity of fired brick samples and on the development of macroscopic defects in the bricks. Saman [28] used percentages from 2.5% to 10% by weight of tea waste to study the compressive strength, water absorption and thermal conductivity of bricks. His results showed that compressive strength and thermal conductivity decreased, while water absorption increased as the percentage of tea residue augmented. Ozturk et al. [29] investigated extruded bricks made with added 10 w% tea waste and fired within a range of 950–1050 °C, whereas in our research, we prepared the samples using the traditional manual kneading method. This produces important differences in the fired bricks. Compared to handmade bricks, extruded bricks show: 1) generally lower porosity and different pore size distribution; 2) more pronounced orientation of flattened minerals, pores and organic fibres (i.e., tea waste). It is also important to take into account the energy cost associated with the use of the hydraulic press to extrude the bricks. For their part, Anjum et al. [30] also produced extruded bricks made with added tea waste fired at temperatures of 600 and 1000 °C. In our opinion, this temperature range does not enable us to fully identify the important mineralogical and textural changes that take place during the firing process in the matrix of the ceramic samples. Other studies mixed ground tea waste with inorganic additives [31] [32]. The particular approach adopted by these researchers made it impossible to assess the impact of the addition of tea waste on certain physical and mechanical properties of the bricks, one of the main objectives of our paper. For example, Sahu et al. [31] used a single firing temperature (990 °C) and were therefore unable to analyse the effects of different firing temperatures on the texture of the fired samples. Similarly, the results obtained by Ibrahim et al. [32] are difficult to compare with ours in that they did not use clay in the brickmaking process, instead mixing varying proportions of tea waste (from 0 to 12 w%) with zeolitic tuff (from 100 to 89 w%).

2. Materials and method

2.1. Geological context and procurement of raw materials

The clayey raw material (with a total mass of over 5 kg) was obtained from a site (lat. 40.311186, long.-1.13375) on the eastern edge of the Betic Cordillera, in the province of Teruel (Spain) (Fig. S1), about 4.2 km from the centre of the city of Teruel. In geological terms, this region is located in the Aragonese Branch of the Betic System [33,34]. The Teruel Basin is the largest Neogene extensional macrostructure within the central-eastern Iberian Chain (NE of Iberian Plate) [35]. The limonitic facies in which the raw material was obtained is made up of clays without exceptional structures, in which there are small sandy layers at the top and high carbonate concentration at the bottom with small subangular quartz grains, traces of K-feldspar, fragments of limestone rocks, fragments of quartzite, silex grains and iron oxides [36]. The quarrying of rock for industrial use is an important sector in this area, involving above all Miocene (Neogene) clays for the brick and ceramic industry (https://igme.es). Within a radius of 2 km around the city of Teruel, there are currently about fifteen quarries producing between 6000 and 18,000 kT of clay per year (*Mining Overview*, Instituto Geológico y Minero de España, IGME 2018–2020, https://igme.es). As regards the tea residue, it came from the tea bags discarded by local households.

2.2. Production of traditional bricks using tea grounds as an additive

The residue from the tea bags (particles from leaves, flowers, small branches, etc.) was mixed and left to air dry for one month at a temperature of approximately 25 °C. The tea residue was not sieved before mixing with the clay to form a kneadable mixture (with 0, 5 or 10% by weight of added tea residue) that ensured homogeneity. Mixing the tea residue with the clay could provide energy savings compared to some of the previous research studies in which the tea residue was milled before mixing. Water was then added until a paste-like texture was achieved. The proportions of raw material, tea residue and water are shown in Fig. 1. The addition of residue meant that less water had to be added to the mixture. We observed that the additive gave the clay mixture a pleasant kneading texture, with a gel-like quality, possibly due to the organic nature of the tea. The clay paste was placed in a previously moistened wooden mould of 15 × 20 × 4 cm and pressed down. Once the mould was full, the surface was smoothed off with a ruler. After one hour, the moulds were removed and the clayey pastes were cut into ~4 cm edge cubes using a stretched cotton thread and left to dry at almost constant room temperature and humidity (20–23 °C, 40–50% RH) for one month.

Once the bricks were dry, they were fired in a Herotec CR-35 electric oven at 800 °C, 950 °C and 1100 °C. Table 1 sets out the acronyms given to the control samples made with no added residue (T0) and to those with added 5 w% (T5) and 10 w% (T10) tea waste. The samples were preheated for 1 h at 100 °C so as to eliminate any residual moisture that might still be present inside them. The temperature was then increased at a rate of 2 °C/min. Once the maximum temperature was reached (800, 950 or 1100 °C), it was maintained for 3 h. Finally, the oven was turned off and the samples were left to cool slowly until the next day, so as to prevent the development of fissures due to the β-to-α quartz transition at 573 °C. After removal from the oven, the bricks were immersed in water for about 1 h so as to prevent possible "lime blowing" due to the presence of lime grains [37].

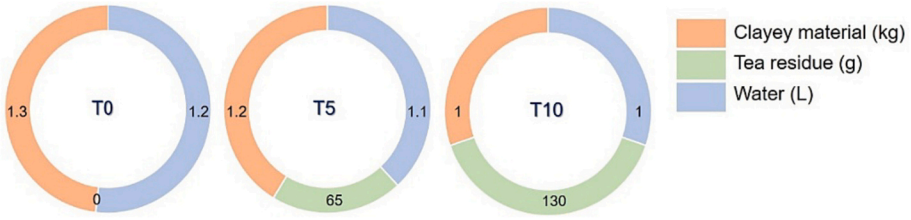

Fig. 1. Amount of clay (kg) and water (L) used in relation to the amount of tea residue added (g).

Table 1
Acronyms assigned to the bricks according to the addition of 0, 5 or 10 w% of tea residue and the firing temperature (800, 950 or 1100 °C).

800 °C	950 °C	1100 °C
T0/800	T0/950	T0/1100
T5/800	T5/950	T5/1100
T10/800	T10/950	T10/1100

2.3. Characterization and testing methods

2.3.1. Chemical, mineralogical and textural study

X-ray fluorescence (XRF) was used to determine the major elements in the raw material and the fired bricks with a PANalytical Zetium compact spectrometer. 3 g of each sample was ground to powder prior to its analysis. The mineralogical composition of the raw clay and the fired bricks was determined by powder X-ray diffraction (PXRD) using a PANalytical X'Pert PRO diffractometer. The working conditions were as follows: CuKα radiation ($\lambda = 1.5405$ Å), 45 kV voltage, 40 mA current, 3 to 70° 2θ exploration range, 0.1 2θ s^{-1} goniometer speed. A first qualitative mineral phase identification was performed using the PANalytical X'pert Highscore Plus 3.0 software matching the experimental diffraction peaks with those included in the Joint Committee for Powder Diffraction Standards (JCPDS) PDF-2 database. A quantitative phase analysis was carried out using open-source Profex-BGMN software with dedicated fitting functions [38] and 10 w% internal standard α-Al_2O_3 was added to the powder samples to comply with the Rietveld refinements [39–41]. The petrographic features (mineralogy, texture and development of vitrification in the matrix) of the samples fired at 800 and 1100 °C were observed by means of polarized optical microscopy (POM). Observations under plane- and cross-polarized light were carried out on polished thin sections using a Zeiss AXIO Scope.A1 microscope equipped with a Canon EOS 550D digital camera. In addition, detailed observations were made on the same thin sections of the samples fired at 800 and 1100 °C using a high-resolution field emission scanning electron microscope (HRSEM) TESCAN SOLARIS coupled with energy dispersive X-ray analysis (EDS). The microscope operated at 5 and 10 kV with a working distance (WD) of 5 mm using a beam current of 300 pA and 1 nA.

2.3.2. Analysis of the pore system

A detailed study of the pore system of the bricks and how it is affected by firing temperature and the addition of tea waste was conducted using several physical tests. Hygroscopic water adsorption and desorption were measured according to the EN-ISO-12571 [42] standard. Brick samples were oven-dried and then placed in an environmental chamber at a constant temperature of 23 °C and with relative humidity (RH) increasing according to the following sequence 30–50–70-75-80-85-90-95% and then decreasing through the same steps in reverse order. The mass of each sample was measured at each step after equilibration at constant RH.

Hydric tests were used to analyse the water flow through the pore network of the bricks. Free (Ab, at atmospheric pressure) and forced (Af, under vacuum) water absorption (UNE-EN 13755 [43]), drying (Di) (NORMAL 29/88 [44]) and capillarity tests (C) (UNE-EN 1926, [45]) were carried out. These tests enabled us to calculate the saturation coefficient (S), the apparent (ρ_a) and real (a_{rc}) densities, and the open porosity (P_o) (UNE-EN 1936, [46]). Hydric tests were performed under controlled thermo-hygrometric conditions (20 °C and 60% relative humidity) using deionized water.

The pore size distribution within a range of 0.002 to 200 mg was analysed by mercury intrusion porosimetry (MIP) using a Micromeritics Autopore IV 9600 porosimeter. Samples of about 1 g were dried in a ventilated oven for 48 h at 30 °C prior to analysis. Apparent and real densities (ρ_{aMIP} and ρ_{rMIP}, g/cm^3), open porosity ($P_{oMIP,}$ %) and specific surface area (SSA, m^2/g) were calculated.

Finally, HRSEM images were analysed using digital image analysis (DIA) in order to estimate the percentage of pores of over 4 μm in size in the bricks with and without tea waste fired at 800 and 1100 °C. For each sample a total of 250 images overlapped by 10% were acquired by the TESCAN SOLARIS using the same working conditions mentioned above and then automatically stitched together in order to cover as much of the thin section as possible, so increasing its representativeness [47,48]. ImageJ software was used to calculate the pore ratio by segmenting and binarizing the BSE images and calculating the ratio of the pixels corresponding to pores to the total area of interest [49]. The resolution limit was 4 μm, the size of one pixel.

2.3.3. Thermal conductivity

A Thermal Conductivity Scanner (TCS) with a Optical Scanning Instrument (OSI) was used to assess the thermal behaviour of the bricks. This high precision noncontact method uses an optical scanning technology based on scanning a sample surface with a focused, mobile, continuously operated heat source in combination with infrared temperature sensors. The thermal conductivity range varied from 0.2 to 25 W/m·K, with an accuracy of 3%. The standards used for calibration were glass (Standard 1) and fused quartz (Standard 2), in line with the components of the bricks. The bricks were painted with acrylic black paint, with a stripe width of approximately 30 mm for each orthogonal side, so as to ensure proper infrared absorption to heat the sample. The thermal diffusivity (α, mm^2/s) of the samples was determined indirectly on the basis of the apparent density values measured by MIP (ρ_{aMIP}) and a mean heat capacity (Cp) value of 800 kJ/g·K established in previous research [50,51].

2.3.4. Compactness and strength

The ultrasound propagation velocity of compressional (V_p) and shear (V_s) waves was performed with a Panametrics HV Pulser/Receiver 5058PR coupled with a EPOCH650® Ultrasonic Flaw Detector (Olympus) performed with transducers of 1 MHz over a circular contact surface of 30 mm in diameterto determine the compactness of the bricks made with and without tea residue. A viscoelastic gel was used to ensure good coupling between transducers and brick samples. V_p and V_s were measured in the three perpendicular directions on three samples per brick type. Once the ultrasound velocities had been determined, we then calculated the Poisson coefficient (ν) and the Young (E), Shear (G) and Bulk (K) moduli.

The compressive strength (Cs) was measured on three samples per brick type according to the requirements of the UNE-EN 196–1 [52] standard. For this purpose, we used a Controls Uniframe T1192

electromechanical universal tester, equipped with 100 kN and 25 kN load cells. Samples with dimensions of 1.5 × 1.5 × 6 cm^3 were tested using a specifically designed device that is mounted on the press.

The PCE-2500 N Leeb Hardness (LH) tester was used to determine whether the surface hardness of the bricks varied in line with the firing temperature or the amount of added residue. The rebound of the hammer was measured in ten different places along a line running from one edge of each brick to the opposite side, passing through the centre.

2.3.5. Colour

The colour of the fired bricks was assessed using a Konica Minolta CM-700d spectrophotometer which quantified their lightness and chromaticity according to the UNE-EN 15886 [53] standard. Illuminant D65, 10° observer and a measurement area of 8 mm were used. Nine measurements per sample were performed to determine their lightness (L*) and chromatic coordinates (a* and b*). Once the L*, a* and b* values had been determined, we then calculated the total colour variation (ΔE) between bricks with and without tea residue as follows (Eq.1):

$$\Delta E = \sqrt{(L_1 - L_2)^2 + (a_1 - a_2)^2 + \left(b^1 - b^2\right)^2} \quad (1)$$

where L_1, a_1 and b_1 are the lightness and chromaticity values for the control bricks made with no added residue and L_2, a_2 and b_2 for those made with added tea waste.

2.3.6. Durability

Fifteen salt crystallization cycles were performed according to the UNE-EN 12370 [54] standard. The objective of this test is to reproduce a decay process that could affect the lifetime of the bricks due to the dissolution and recrystallization of soluble salts within their porous systems. Three samples (4 cm-edge cubes) per brick type were used for this test. To further determine the effect of the salts on the pore system of these samples, ultrasound measurements were carried out before the decay test and after the 4th, 10th and 15th cycles.

3. Results and discussion

3.1. Changes in the weight of the bricks after firing

As expected, the difference in weight between unfired and fired bricks varies according to the amount of tea residue added and the firing temperature. i.e., the larger the amount of residue added and the higher the firing temperature, the greater the difference in weight between the fired and unfired bricks (Table S1). The bricks made with added waste are lighter. The highest weight change was measured in T1100/10 for which a weight loss of about 30% was observed. This trend is in line with the findings of other authors, who reported a decrease in the weight of the samples made with added organic matter after firing [26,55,56].

3.2. Chemical, mineralogical and textural study

3.2.1. X-ray fluorescence (XRF)

Table 2 shows the chemistry of the raw material and the fired bricks. The main difference is that the fired bricks have lower Loss on Ignition (LOI) values. This is because the organic matter present in the raw material is consumed during firing, and the carbonates decompose, as manifested by the ~8% of CaO identified. The dehydroxylation of phyllosilicates will also have influenced the decrease in the LOI value. LOI increases in line with the amount of tea residue in the bricks ($LOI_{T0} < LOI_{T5} < LOI_{T10}$). However, with firing temperature the opposite occurs. LOI falls as firing temperature increases. Chemically, the raw material and the bricks are rich in silica and alumina suggesting the presence of quartz and aluminium silicates. Based on its CaO content, the raw material can be classified as calcareous [57]. Iron compounds are the fourth most abundant with values of between 3.8 and 4.1% and their presence enables the formation of iron oxides. Finally, K_2O makes up around 2–2.5% and seems linked to the formation of feldspars and phyllosilicates, while the remaining elements account for <1%.

3.2.2. Powder X-ray diffraction (PXRD)

The Rietveld refinement of the PXRD analysis reveals that the raw material is mainly composed of quartz (64.78 w%). Calcite, phyllosilicates (illite and kaolinite), K-feldspar and hematite were also identified (Table 3). The clay has an amorphous phase content of 8.46 w%, which can be attributed to the presence of organic matter. Fig. S2 shows the changes in the mineralogy of the bricks after firing, which are more evident at 1100 °C with the crystallization of high-temperature silicates and an increase in the background noise due to the vitrification of the samples [37,58]. The amorphous phase content (in w%) increases in line with the firing temperature and with the percentage of tea residue added, reaching its highest value in the samples fired at 1100 °C and with 10 w% waste. It is possible that the tea residues generate additional heat, which results in a more pronounced vitrification of the matrix. If we look at the results in more detail, at the three firing temperatures investigated (800, 950 and 1100 °C), quartz is the most abundant phase although its concentration drops sharply when the firing temperature reaches 1100 °C and as the amount of residue increases, with values ranging from 45 to 27 w% (Table 3). The lower quartz values at 1100 °C suggest that at this temperature, some of the quartz has been consumed in mineralogical reactions to form new high-T silicate phases. At 800 °C, dehydroxylated illite-type phyllosilicates are still present (Fig. S2), albeit in lower amounts compared to the raw material, while the kaolinite has decomposed (Table 3). Calcite is detected in smaller amounts compared to the raw material and disappears at higher temperatures (Fig. S2 and Table 3). The microcline detected in the raw material is converted into more stable polymorphs, i.e. orthoclase at 800 °C and sanidine at 950 °C and 1100 °C [59,60]. Hematite is detected in all the samples, irrespective of the amount of tea residue added. It has a higher concentration in the bricks fired at 800 °C than in the clay raw material due to the decomposition of the phyllosilicates, which favours the recrystallisation of Fe in the matrix. At higher temperatures, the

Table 2
XRF results (in %) for the raw material and for the fired bricks.

	SiO_2	Al_2O_3	Fe_2O_3	MnO	MgO	CaO	Na_2O	K_2O	TiO_2	P_2O_5	LOI	Total
Raw material	65.72	9.40	3.77	0.06	0.69	7.85	0.11	2.21	0.52	0.12	9.52	99.97
T0/800	73.18	9.28	3.8	0.05	0.66	6.98	0.11	2.19	0.54	0.12	3.07	99.98
T5/800	69.39	10.40	4.11	0.07	0.78	8.53	0.12	2.44	0.63	0.15	3.36	99.98
T10/800	68.43	10.13	3.95	0.07	0.78	8.75	0.12	2.46	0.60	0.17	4.53	99.99
T0/950	73.10	9.88	4.02	0.06	0.72	7.62	0.12	2.32	0.56	0.14	1.44	99.98
T5/950	71.84	10.07	4.08	0.07	0.77	7.98	0.13	2.43	0.56	0.16	1.90	99.99
T10/950	70.61	10.39	4.10	0.07	0.82	8.46	0.13	2.60	0.59	0.19	2.01	99.97
T0/1100	73.39	10.08	4.09	0.06	0.73	8.04	0.12	2.34	0.57	0.13	0.44	99.99
T5/1100	73.21	9.70	3.91	0.06	0.73	7.92	0.12	2.44	0.59	0.15	1.16	99.99
T10/1100	70.69	10.73	4.18	0.07	0.84	9.33	0.13	2.59	0.62	0.18	0.63	99.99

Table 3
Mineralogical characterization by XRD of the clayey material and the fired bricks with or without tea residue. Data is provided in weight %. Abbreviations of minerals according to Warr [64]: Qz: quartz; Kln: kaolinite; Cal: calcite; Ilt: illite; Hem: hematite; Mc: microcline; Or: orthoclase; Sa: sanidine; An: anorthite; Aug: augite; Gh: gehlenite; Wo: wollastonite; AM: amorphous phase.

	Qz	Kln	Cal	Ilt	Hem	Mc	Or	Sa	An	Aug	Ghl	AM	ERROR
Clayey material	64.78	4.30	6.65	11.81	2.08	1.90	0	0	0	0	0	8.46	±0.96
T0/800	44.04	0	6.91	9.88	4.8	5.66	0	0	0	0	0	28.61	±1.11
T5/800	35.48	0	5.25	13.71	5.82	0	3.01	0	0	0	0	36.72	±2.13
T10/800	33.76	0	5.04	10.67	6.01	0	1.88	0	0	0	0	42.67	±3.12
T0/950	45.13	0	0	0.20	4.52	0	0	1.78	5.12	0	7.14	31.54	±1.63
T5/950	43.15	0	0	2.00	4.93	0	0	2.36	5.77	0	6.04	36.17	±1.06
T10/950	36.34	0	0	0	3.44	0	0	3.64	6.06	0	7.23	44.41	±2.41
T0/1100	40.33	0	0	0	3.91	0	0	2.31	8.34	4.19	5.64	35.24	±1.99
T5/1100	34.24	0	0	0	1.40	0	0	2.74	9.65	5.40	4.22	42.65	±1.78
T10/1100	26.78	0	0	0	0.68	0	0	3.59	10.54	5.88	4.07	48.74	±3.82

hematite content falls to its lowest value of 0.78 w% in the T10/1100 sample (Table 3). This is because iron is trapped inside the structure of the new silicates, so hindering the formation of hematite [37,61–63]. The decomposition of carbonates and their reactions with quartz and other silicates leads to the appearance of new Ca-silicates such as gehlenite at 950 °C and wollastonite and anorthite at 1100 °C.

3.2.3. Polarized optical microscope (POM)

Polarized optical microscopy (POM) observation of the T0/800 control bricks (samples with no added waste fired at 800 °C) revealed the presence of quartz grains with undulose extinction of over 1 mm in length in an orange-to-brown coloured matrix (Fig. 2A), which turns black in the bricks fired at 1100 °C (T0/1100) (Fig. 2D). Higher porosity was observed in the bricks with added tea residue (Fig. 2B, C, E and F), in which this organic matter disappears after combustion leaving imprints in the form of pores. The porosity increases in line with the percentage of residue (T5/800 and T10/800, Fig. 2B and C). The addition of tea residue also seems to affect the colour of the matrix, such that in the bricks made with 5 and 10 w% tea residue, the matrix is darker than in the control sample (T0/800). In addition to the quartz, calcite, phyllosilicates (muscovite-type) and feldspar grains were also identified. Phyllosilicates and elongated fragments of other minerals often show a preferential orientation due to the pressure exerted on the raw material during the kneading process. Muscovite-type crystals appear unaltered reaching a second-order interference colour. The carbonate grains are partially decomposed and have lost their typical high birefringence colour. At 1100 °C, the bricks undergo major textural changes due to the high firing temperature (Fig. 2D, E and F), the pores become ellipsoidal-to-rounded in shape and the matrix becomes darker and loses its birefringence due to vitrification. Only quartz grains can be identified.

3.2.4. HRSEM

The textural features of the bricks vary considerably according to their firing temperature (800 and 1100 °C) and tea residue content (0, 5 or 10 w%). Both these factors alter the texture by improving the interconnection between mineral grains and increasing the porosity. These differences are reported in Fig. 3 where SEM-BSE images show changes in the structures due to the firing process, such as the high sintering in sample T5/1100 due to the addition of tea residue. In samples fired at 800 °C, there are large gaps/pores between the grains. The pores are irregular in shape and clay minerals are still evident in the groundmass (Fig. 3A). Nuclei of new silicates phases are also present in the matrix of the bricks fired at 800 °C with 5 and 10 w% of tea waste (Fig. 3B and C). Even though they were not detected by PXRD due to their small quantities, their presence indicates a higher level of sintering as a result of the addition of tea residue, as suggested by the increased amorphous phase revealed by the Rietveld refinements (see Table 3). Reaction rims, in particular on the edges of the quartz grains, are frequent (Fig. 3D). Fibrous phytoliths resulting from the addition of tea residues have been observed in bricks fired at 800 °C, where amorphous silica reacts with

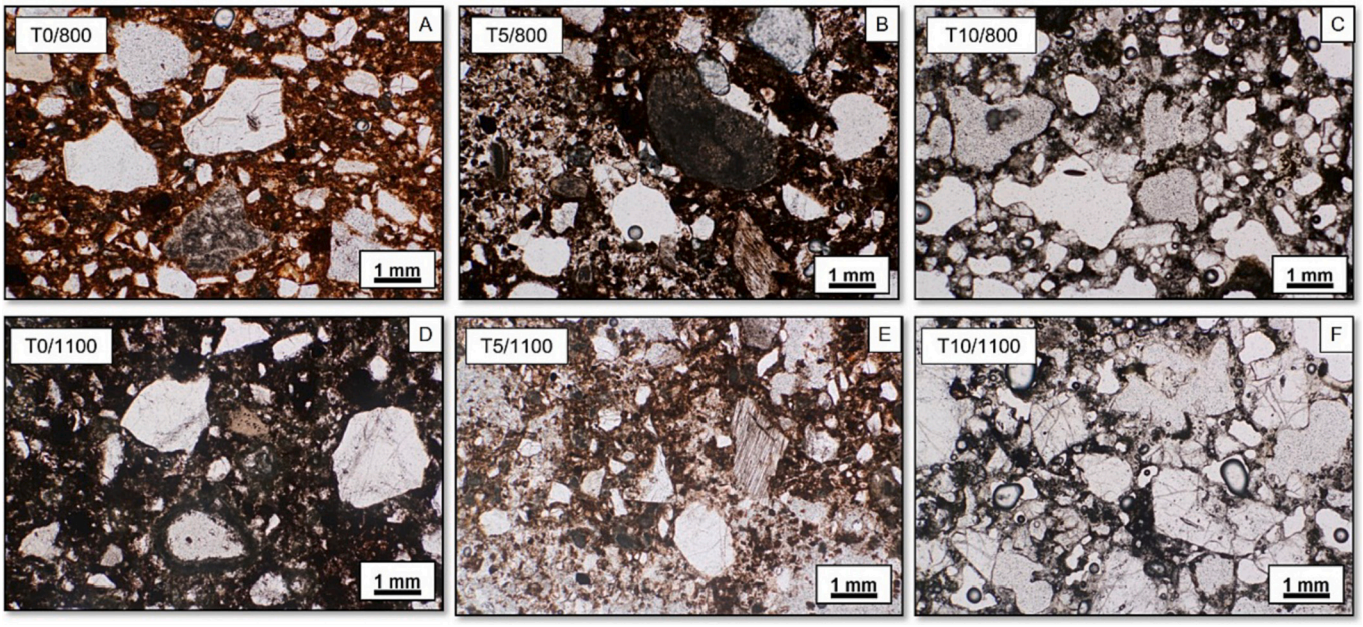

Fig. 2. Bricks with and without added tea residue fired at 800 and 1100 °C. All photographs were taken with plane-polarized light (PPL).

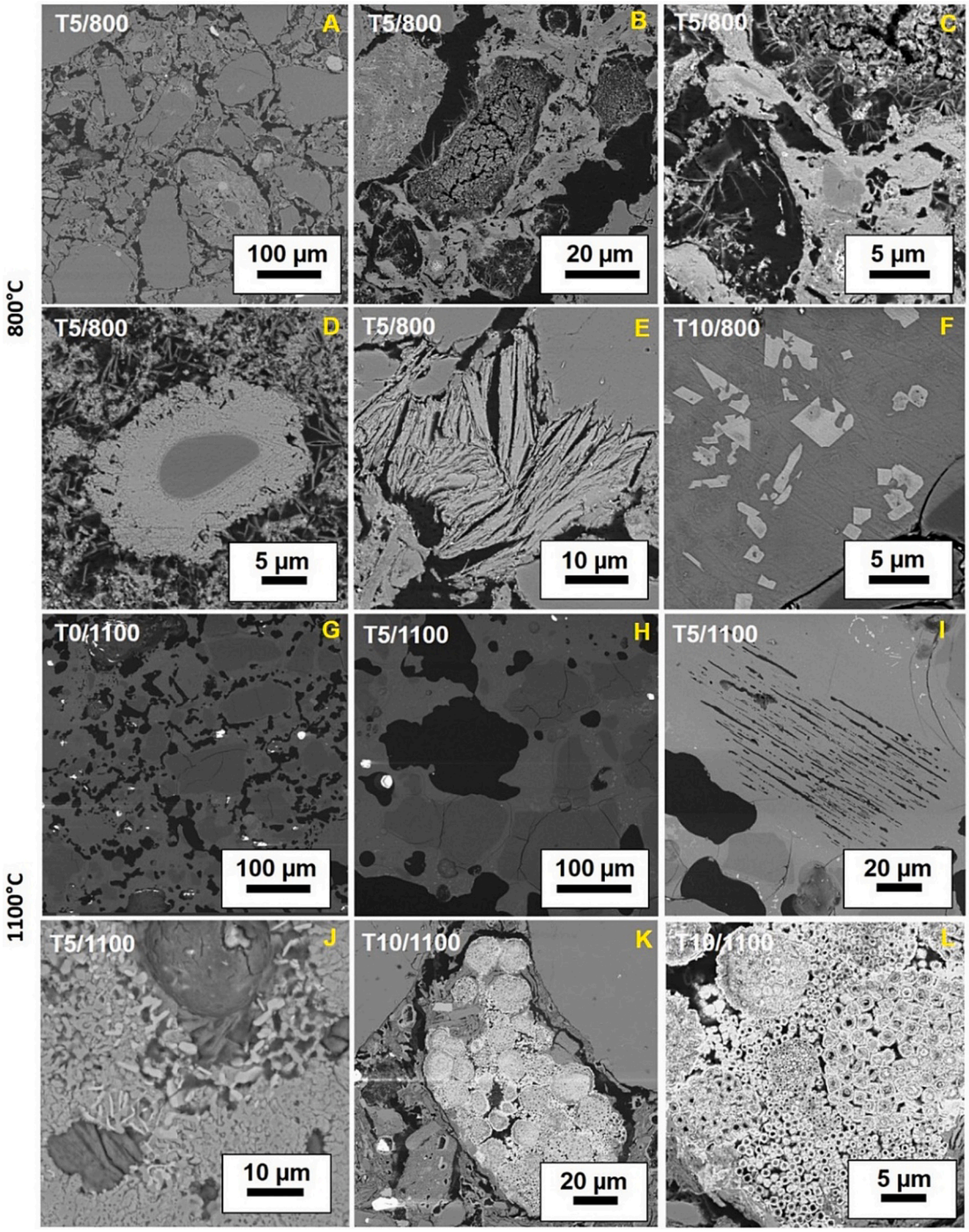

Fig. 3. High resolution SEM-BSE images of bricks made with and without added tea residue fired at 800 and 1100 °C.

residual calcite grains [65], (Fig. 3E). This supports the mineralogical process in which new silicates are formed.

In the samples fired at 1100 °C, the illite has decomposed completely and melted in a highly sintered matrix, which displays the growth of new silicates and the development of larger, rounded pores (Fig. 3G and H). Reaction rims on the edges of the quartz grains are also frequent at this temperature (Fig. 3J). Framboidal hematite, with microcrystallites of between 0.5 µm and 5 µm in diameter, was found in some bricks (Fig. 3K and L). The framboidal texture suggests that they were pyrite crystals, which probably formed due to the presence of organic matter [66,67,68] and the establishment of an anoxic environment that enhanced the activity of sulphate-reducing bacteria [60,69]. During the firing of the bricks, the sulphur content of the framboids fell due to the decomposition of these sulphides at 588 °C and, in an oxidising atmosphere, were transformed into Fe_2O_3 [70].

The chemical composition maps (area and linear) in Fig. 4 reveal the growth of new Ca-silicate phases (mainly wollastonite and maybe gehlenite) close to quartz and calcite grains.

3.3. *Pore system*

As regards the interaction of the bricks with water vapour and their behaviour with respect to RH variations, Fig. 5 shows that the bricks fired at 800 °C adsorb more vapour than those fired at higher

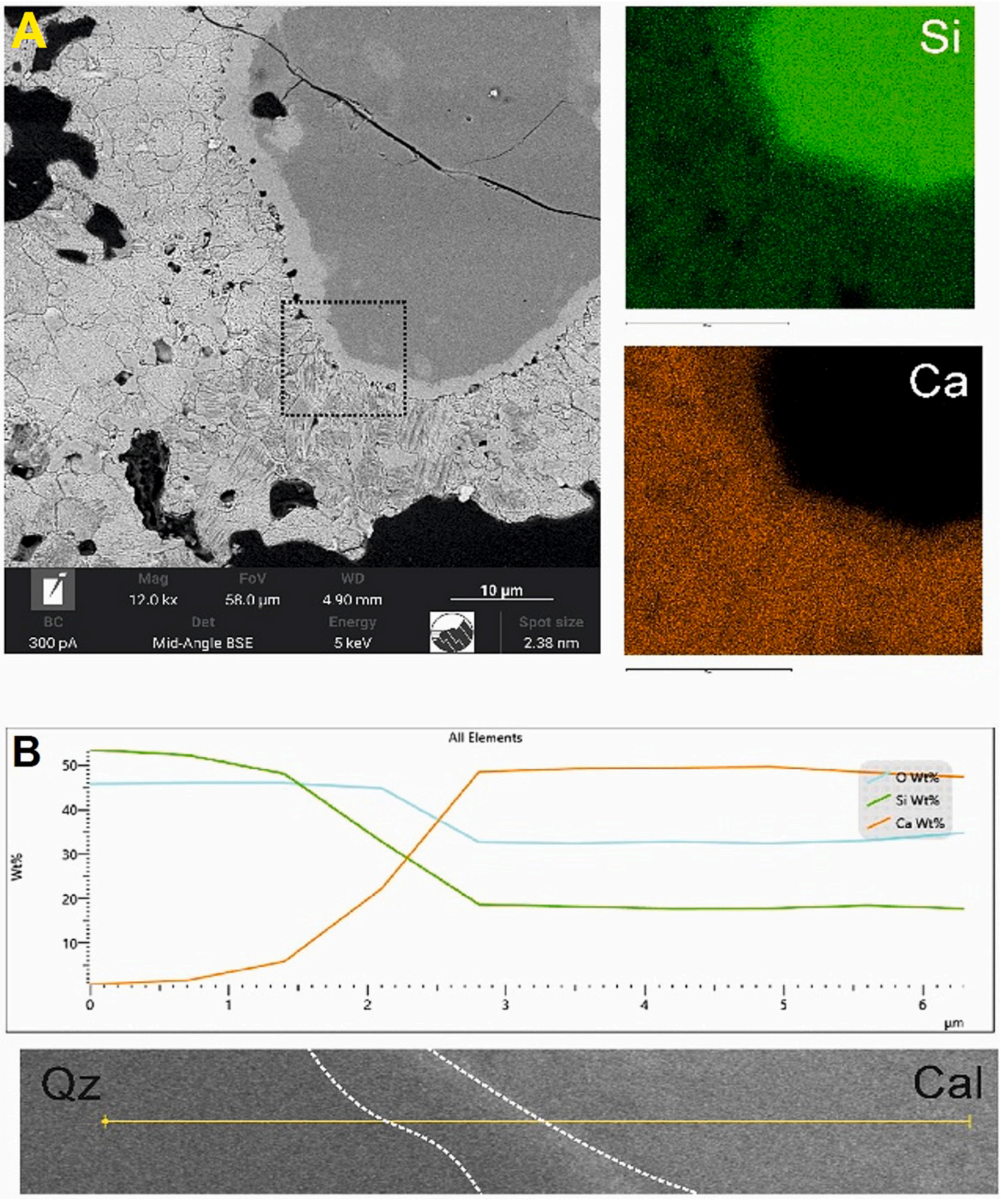

Fig. 4. A) SEM-EDS elemental maps and B) a linear chemical analysis along a reaction rim between quartz and calcite grains.

temperatures. As for the tea residue, the samples with higher amounts of additive are those in which mass increases most, because they have more empty spaces and are able to absorb more water vapour. The samples fired at 800 °C experienced the greatest increase in mass of around 3–3.5%, values that were reached at 90–95% RH. The mass of these samples increased progressively, as RH increased from 30 to 90–95% and then went down again as RH went back to 30%, still retaining some moisture at the end of the test. In the samples fired at 1100 °C, the mass

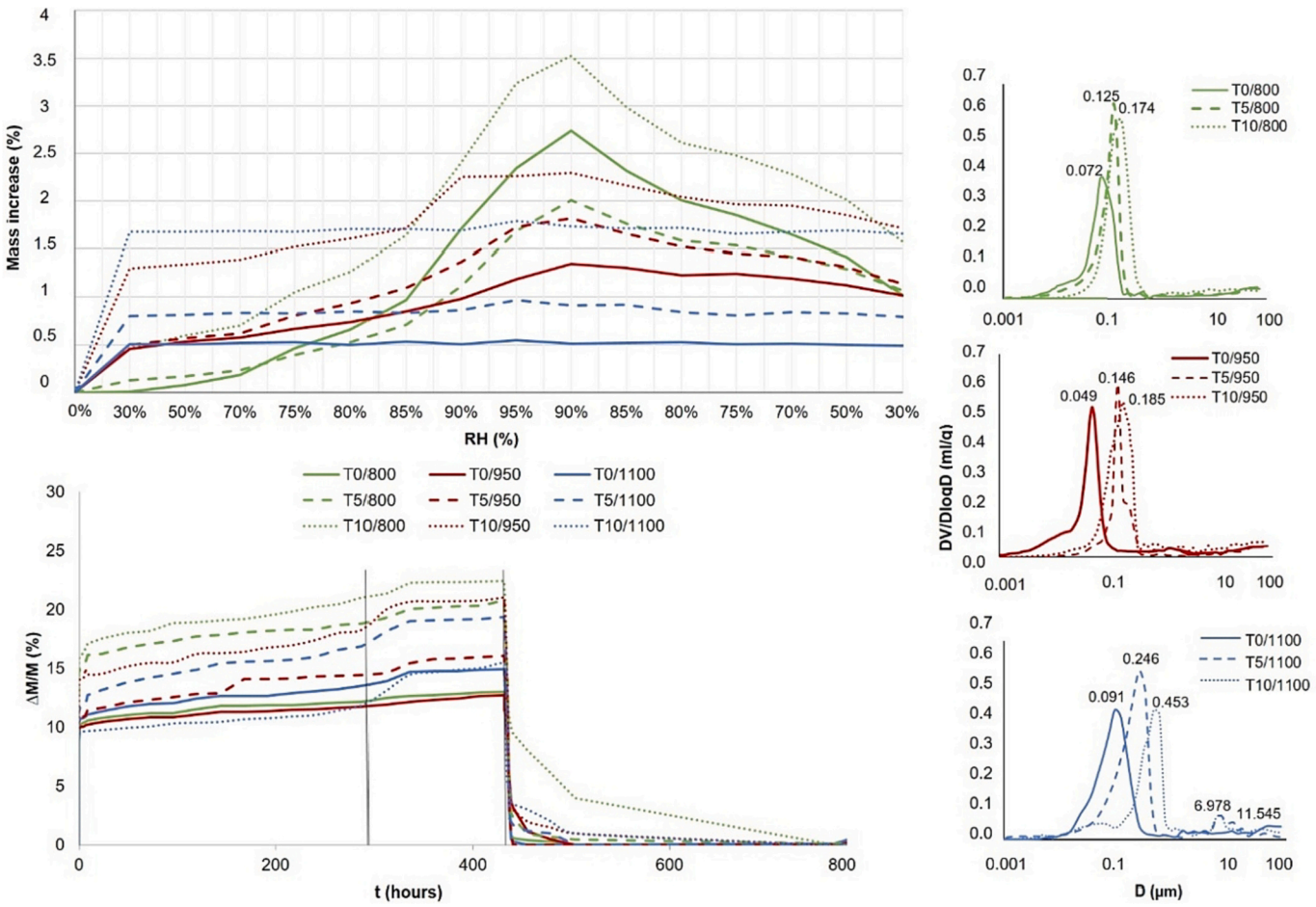

Fig. 5. Interaction of the bricks with water vapour and their behaviour in relation to RH variations (mass increase versus relative humidity both in %), hydric behaviour of the bricks (weight variation in % versus time in hours) and MIP curves (frequency in % versus pore diameter in μm) for bricks fired at 800, 950 and 1100 °C with no additive (continuous line) and with added tea residue (dashed lines).

only increased during the first cycle (from 0 to 30% RH) and thereafter remained almost stable (Fig. 5).

As regards the hydric tests on the bricks, the porosity and water absorption of the bricks increase in line with increasing amounts of tea residue (Fig. 5 and Table 4). This indicates that the hydric behaviour of the bricks is more affected by the addition of tea residue than by the firing temperature. At 800 °C, Ab increases from 12.9% (T0) to 22.4% (T10) (Table 4). The same trend is observed with forced water absorption (Af, Table 4). The interconnection between the pores improves (i.e., Ax values decrease) and open porosity augments (Po, Table 4) as the amount of tea residue increases, so making the bricks more absorbent (S, Table 4). Ax and Po values are more or less the same for each group of bricks (T0, T5 and T10) at the three firing temperatures. As for capillarity (C, Table 4), the bricks tend to absorb water more slowly as the amount of tea residue increases. The control bricks have the highest C values. This is because the capillaries are larger in the bricks with added organic matter, so hampering capillary rise [26,71]. The increase in the amount of tea residue always leads to a decrease in apparent density (ρ_a, Table 4). There is less variation in real density (ρ_r), which is mainly influenced by the mineralogy of the bricks.

MIP analysis revealed that the addition of tea residue alters the pore size distribution in the bricks. All the bricks show a unimodal pore size

Table 4
Hydric, MIP and DIA parameters for bricks with and without tea residue. Ab: free water absorption (%); Af: forced water absorption (%); Ax: degree of pore interconnection (%); S: saturation coefficient (%); Di: drying index. P_o: open porosity by hydric test (%); C: capillarity coefficient (g/m^2s^{05}); ρ_a: apparent density (g cm^{-3}); ρ_r: real density (g cm^{-3}). Po_{MIP} = open porosity by MIP (%); ρ_{aMIP} = apparent density (g cm^{-3}); ρ_{rMIP} = real density (g cm^{-3}); SSA = specific surface area (m^2/g); Po_{DIA} = open porosity by DIA (%); MinFeret = the largest MinFeret diameter measured by DIA.

	Hydric behaviour									MIP				DIA	
	Ab	Af	Ax	S	Di	Po	C	ρ_a	ρ_r	Po_{MIP}	ρ_{aMIP}	ρ_{rMIP}	SSA	Po_{DIA}	MinFeret
T0/800	12.94	13.01	11.46	85.12	1.30	40.56	3.80	1.92	3.06	36.47	1.54	2.42	10.06	11.18	1386
T5/800	20.34	20.76	8.90	91.88	2.07	44.91	3.59	1.65	2.88	39.67	1.44	2.39	3.72	19.96	1382
T10/800	22.37	22.42	6.28	93.74	2.24	48.67	3.11	1.55	2.53	46.53	1.36	2.55	2.09	32.89	3529
T0/950	12.68	12.73	11.25	86.46	1.27	42.34	3.56	1.69	2.19	41.43	1.96	1.98	9.72	–	–
T5/950	15.94	16.05	7.75	93.46	1.60	45.70	2.91	1.09	1.94	44.44	1.66	1.99	2.8	–	–
T10/950	20.78	21.02	5.30	94.65	2.10	49.03	2.14	0.92	1.48	51.61	1.14	1.35	1.49	–	–
T0/1100	14.87	14.87	12.95	82.07	1.49	42.81	3.82	1.53	2.40	41.97	1.63	2.81	8.44	14.56	1141
T5/1100	19.20	19.38	6.11	93.34	1.93	44.46	2.46	1.21	2.16	47.12	1.45	2.74	1.43	34.24	3513
T10/1100	15.05	15.46	5.08	95.97	1.54	49.22	1.98	0.98	2.64	54.11	1.51	3.09	1.22	38.92	13,153

distribution with a maximum peak at around 0.1 μm in bricks fired at 800 °C and 950 °C and 0.2 μm in those fired at 1100 °C. The addition of residue causes the main peak to shift to the right of the diagrams, i.e. towards higher pore sizes. This is most evident at 1100 °C where the peaks for T5/1100 and T10/1100 are at 0.25 and 0.45 μm, respectively. At 1100 °C, a second family of pores can be clearly distinguished at around 10 μm (Fig. 5). The open porosity is influenced by the addition of residue, so confirming the results of the hydric tests (P_{oMIP}, Table 4).

Digital image analysis (DIA) was performed on the two sets of samples fired at 800 °C (T0/800, T5/800, T10/800) and 1100 °C (T0/1100, T5/11000, T10/1100) (Table 4). This highlighted the increase in both porosity and pore size in line with the increase in firing temperature and in the percentage of tea residue added, so confirming the qualitative observations reported in Sections 3.2.3 and 3.2.4. The abundance of pores of over 4 μm explains the differences observed in the weight of the bricks after firing (Table S1). The pores were also affected by the addition of tea waste, as is clear in the samples fired at 800 °C where porosity increased in line with the tea percentages, from 11.18% (T0/800) to 19.96% and 32.89% (T5/800 and T10/800, respectively). A large difference was noted in the bricks fired at 1100 °C. The high firing temperature increased the porosity [72,73], as confirmed by the T0/1100 sample, which had 20% more pores than the T0/800 sample. At 1100 °C, the addition of tea waste caused a significant increase in porosity from 14.56% to 34.24% and 38.92% for T5/1100 and T10/1100, respectively. The combined effects of firing temperature and tea waste addition are also detectable in pore size analysis. Table 5 sets out the maximum and minimum diameter found in each section in terms of caliper diameter (MinFeret) [47,48], which increases in line with increasing firing temperature and tea waste percentage. While the samples T0/800, T5/800, and T0/1100 display the largest minFeret of about 1100–1300 μm and the samples T10/800 and T5/1100 show a minFeret of around 3500 μm, the sample fired at 1100 °C made with 10% of tea residue (T10/1100) has pores with a minFeret of just over 13,000 μm (i.e., >1 cm).

3.4. Thermal conductivity

The results of the thermal conductivity measurements are shown in Table 5. Values measured on the three orthogonal directions revealed that the thermal behaviour of the bricks is anisotropic. This is due to the brickmaking process applied here, which was based on the traditional method of pressing and moulding by hand (a = perpendicular to the pressure exerted, b and c = parallel to the pressure exerted). The highest values were found normal to the side of brick (λ(c)), while λ(a) and λ(b) showed similar thermal conductivity values, which were about 10% lower than for (λ(c)). The mean thermal conductivity (λmean) ranges from 0.34 to 0.91 (W/(m·K)), in accordance with the findings of previous research [25,51,74,75]. Values decrease in line with the increase in temperature from 800 °C to 1100 °C and with the increase in tea residue content (0, 5 or 10 w%), suggesting a direct relationship between λ and porosity [75,76]. When thermal conductivity is plotted against porosity (Fig. S3), an $R^2 > 0.8$ is found. The best correlation was obtained by the hydric test analysis of open porosity (Po, Table 4) ($R^2 = 0.9552$), in which a medium-sized pore range was observed, as compared to the smaller sizes measured by MIP ($R^2 = 0.8061$) and the larger ones recorded by DIA ($R^2 = 0.8864$) (Fig. S3).

The estimated heat diffusivity α also decreases with an increase in firing temperature and in tea waste content. α varied from $2.01 \cdot 10^{-7}$ mm/s and $2.87 \cdot 10^{-7}$ mm/s for samples with 10 w% of tea residues to $3.71 \cdot 10^{-7}$ mm/s to $4.89 \cdot 10^{-7}$ mm/s for samples with no added tea residue. Those with 5 w% of added residue obtained intermediate values for all three firing temperatures (Table 5). These results indicate that the addition of tea residue strongly decreases both thermal conductivity and heat diffusion capacity, suggesting that bricks made with this additive would have good thermal insulation properties.

Table 5
Thermal behaviour: λ(a), λ(b) and λ(c) = thermal conductivity measured normal to the sides a (perpendicular to the pressure exerted), b and c (parallel to the pressure exerted) of the sample (W/(m·K)); λ_{mean} = mean thermal conductivity (W/(m·K)) calculated on the three sides λ(a), λ(b) and λ(c); α = thermal diffusivity calculated by λ_{mean} (mm/s).

	$\lambda_{(a)}$	$\lambda_{(b)}$	$\lambda_{(c)}$	λ_{mean}	A
T0/800	0.83	0.89	1.01	0.91	$3.71 \cdot 10^{-7}$
T5/800	0.64	0.68	0.75	0.69	$3.01 \cdot 10^{-7}$
T10/800	0.45	0.47	0.48	0.47	$2.32 \cdot 10^{-7}$
T0/950	0.76	0.82	0.99	0.85	$4.89 \cdot 10^{-7}$
T5/950	0.53	0.60	0.72	0.61	$3.97 \cdot 10^{-7}$
T10/950	0.32	0.33	0.37	0.34	$2.87 \cdot 10^{-7}$
T0/1100	0.75	0.83	0.84	0.81	$4.20 \cdot 10^{-7}$
T5/1100	0.56	0.63	0.68	0.62	$3.62 \cdot 10^{-7}$
T10/1100	0.35	0.43	0.49	0.42	$2.01 \cdot 10^{-7}$

3.5. Compactness and strength

The control bricks (T0) show higher compressive strength than those with added tea residue (T5 and T10), which is logical considering the large number of new pores formed in the T5 and T10 bricks after the combustion of the organic matter during firing (see Po, Table 4). The sample with the highest compressive strength was T0/1100 (29.3 MPa, Fig. 6). If we look at the three groups of samples with 0, 5 and 10 w% of tea residue, the bricks fired at 1100 °C always had the highest compressive strength values (Fig. 6), due to their higher level of vitrification, as was demonstrated by PXRD analysis and microscope observations. These results are in line with those of previous research studies in which it was found that compressive strength is more closely related with porosity and the degree of vitrification of bricks than with the mineralogy of the raw material [37,72,77,78]. In a similar trend to compressive strength, the highest surface hardness values were observed in the bricks with no tea residue fired at 950 and 1100 °C (385.7 and 446.8, respectively) (Fig. S3). In all the bricks, the higher the amount of tea residue added, the lower the surface hardness. The lowest hardness values were obtained in the bricks fired at 800 °C and with 10 w% tea residue. These were 34% lower than those made without the additive and fired at the same temperature. However, according to official specifications from the Spanish Ministry of Public Works (Pliego RL-88) [79], the minimum compressive strength value for bricks to be used in the construction industry is 10 MPa. All the samples obtained compressive strength values above this threshold, so making them suitable for use as building materials.

Table 6 shows the average values for ultrasound velocities (V_p and V_s) measured in bricks made with and without tea residue. The highest V_p and V_s values were measured in bricks fired at 1100 °C. The increase in velocity is not gradual from 800 to 1100 °C, in that V_p and V_s are similar at 800 and 950 °C. In some cases (when residue is added) they are lower at 950 °C and experience a significant rise at 1100 °C. The higher velocity is a sign of greater compactness [72]. This indicates that vitrification occurs more between 950 and 1100 °C than between 800 and 950 °C. The formation of new pores due to use of added tea waste results in a decrease in V_p and V_s. The lowest ultrasound value was for the samples fired at 950 °C with 10 w% residue (Table 6). In this case, it is possible that the combustion of organic matter together with the total decomposition of the calcite grains and the higher phyllosilicate dehydroxylation at 950 °C reduced the compactness of the bricks compared to those fired at 800 °C.

The Poisson's ratio (ν) values are very similar for all the samples regardless of the firing temperature or the addition or not of tea residue. The mean values of around 0.30 indicate a value similar to that of shale, a sedimentary rock with a mineralogy comparable to that of bricks [80]. This value decreases slightly for bricks with added tea residue (about 0.27, Table 6), a value closer to silty materials, loose sands or soft clays [81]. The Young (E), shear (G) and bulk (K) moduli (Table 6) decrease in

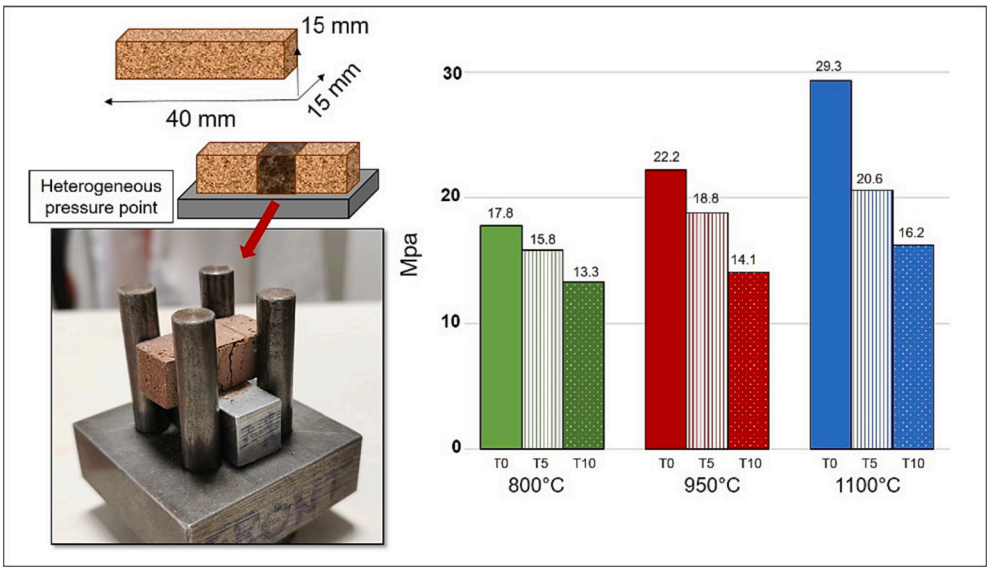

Fig. 6. Mechanical behaviour for bricks fired at 800, 950 and 1100 °C made without additives (control group, T0) and with added tea residue (T5 and T10).

Table 6
Average velocities for the propagation of ultrasonic V_P and V_S (in m/s). ν: Poisson's ratio; E: Young's modulus (in GPa); G: shear modulus (in GPa); K: bulk modulus (in GPa).

	Mean V_P (m/s)	Mean V_S (m/s)	ν	E (x 10^3)	G (x 10^3)	K (x 10^3)
T0/800	2357	1212	0.31	7.39	2.82	0.93
T5/800	2125	1011	0.28	4.34	1.69	0.64
T10/800	1861	939	0.27	2.55	1.00	0.39
T0/950	2443	1238	0.31	6.79	2.59	0.86
T5/950	2101	995	0.30	2.81	1.07	0.37
T10/950	1581	753	0.28	1.34	0.52	0.19
T0/1100	2526	1292	0.32	6.74	2.55	0.81
T5/1100	2346	1088	0.27	3.64	1.43	0.56
T10/1100	2221	1156	0.26	3.30	1.30	0.53

line with the increases inthe amount of tea residue.

3.6. Colour

The colour of bricks is the result of a combination of factors such as the temperature, the type of raw material used (in particular the presence and concentration of Fe oxide, which gives the bricks their reddish colour [82,83]) and the addition of residue. These factors determine the final shade and hue of the samples. During firing, our brick samples underwent certain changes in colour.

The bricks fired at 800 °C are red and have some of the highest a* and b* values (Fig. S4). Higher firing temperatures tend to result in darker shades. The chromatic values and the lightness (L*) tend to decrease in bricks without residues. It is interesting to note that L* is higher for bricks without residues, e.g. at T0/800, L* = 54.25, going down to 43.47 at T10/800.

At 1100 °C, bricks without additive (T0) reach mean values of 11.75 (a*) and 19.24 (b*). The addition of 10% wt. of tea residue results in bricks with a lighter colour (Table S2). The general trend in lightness (L*) is related to the amount of tea residue added, and is higher in the residue-free bricks fired at 800 and 950 °C (T0/800: 54.25 and T0/950: 56.24) than in the T10/800 samples (43.47). The samples fired at 800 and 950 °C have a rough appearance, with numerous pores (Fig.S4) and an orangey shade of red. As the firing temperature increases to 1100 °C, the difference in colour between the bricks produced with and without the addition of tea residue becomes more pronounced. By contrast, the lightness values are more similar.

3.7. Durability

During the salt crystallization test, all the samples gain weight. This is because of the deposition of sodium sulphate inside the pores and fissures of the bricks (Fig. 7A). At the beginning of this ageing test, the weight increase varies from one type of brick to another, with the greatest increases being observed in those with 10 w% tea residue (T10/800, T10/950 and T10/1100). This confirms the results of the hydric tests in which the bricks without residue gained the least weight. This is because less saline solution can enter the pore system and damage the bricks. As the ageing test progresses, small fluctuations of the curves can be observed with increases and losses in weight which are linked respectively to the crystallization of the salt in new fissures and the consequent loss of fragments due to crystallization pressure. Using ultrasound, we were able to monitor the behaviour of the bricks during the salt crystallization decay test (Fig. 7b). Again, the P waves move faster in the bricks without additives and slower in those with 10 w% residue. Over the course of the test, all the samples showed an increase in the average wave velocity, which was especially evident after the 4th cycle, because of the crystallization of salts in the pores of the bricks.

4. Conclusions

In this paper, chemical, mineralogical and physical techniques were applied to assess the behaviour of solid bricks that were handmade with a clayey raw material from Teruel (Spain) to which 0, 5 or 10 w% of tea waste was added. The samples were fired at temperatures of 800, 950 and 1100 °C. The following conclusions were reached:

- Tea residue did not affect the mineralogy of the bricks. The mineralogical changes that occurred during firing were dependent on the raw material and the firing temperature, with higher temperatures leading to increased amounts of amorphous phase due to the vitrification of the brick matrix.
- The tea waste had a more significant effect on the hydric behaviour of the bricks than the firing temperature, increasing porosity and water vapour absorption in proportion to the amount of added residue. This is because the residue is consumed during firing, creating more empty spaces.
- Mercury intrusion porosimetry and digital image analysis highlighted that pore sizes and porosity increased in line with increases in the amount of added waste and in firing temperature.

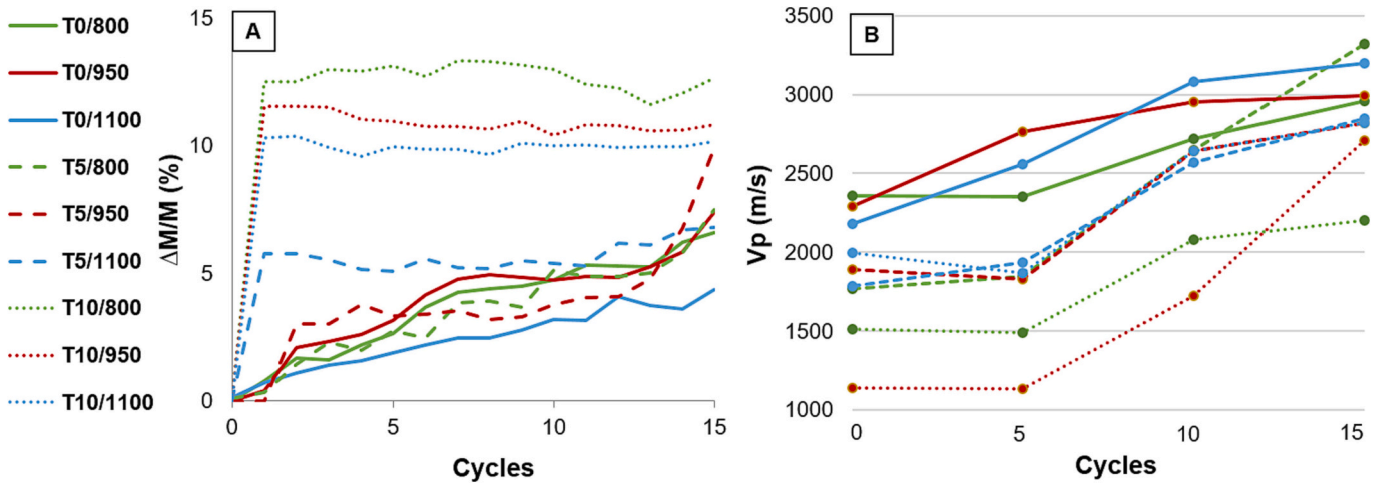

Fig. 7. A) Weight variation in the bricks made without additives (T0) and with added tea residue (T5 and T10) over 15 salt crystallization test cycles. Each curve represents the mean of three measurements. B) V_P velocities during the salt crystallization test for bricks fired at 800, 950 and 1100 °C without additives and with added tea residue.

- The addition of tea waste reduced thermal conductivity and heat diffusion in the bricks, making them suitable for thermal insulation.
- The bricks made without added waste were mechanically stronger than those made with the additive, but both comply with the specifications required by the construction industry.
- The addition of tea waste created new pores, so reducing ultrasound velocities. This indicates a reduction in the compactness of the bricks. The higher the amount of added residue, the lower the velocity.
- The addition of tea waste gave the bricks a more greyish colour, decreasing the lightness and the chromaticity parameters.
- In terms of durability, the bricks made with the highest amount of tea waste (10 w%) undergo the greatest variation in weight due to salt crystallization regardless of the firing temperature. The bricks with no added waste or with 5 w% showed similar decay behaviour. Therefore, the addition of this percentage of waste does not reduce the durability of the bricks when exposed to salt crystallization.

CRediT authorship contribution statement

Laura Crespo-López: Visualization, Validation, Software, Methodology, Investigation, Formal analysis, Conceptualization, Writing – review & editing, Writing – original draft. **Chiara Coletti:** Supervision, Investigation, Data curation, Writing – review & editing. **Anna Arizzi:** Visualization, Resources, Project administration, Funding acquisition, Writing – review & editing. **Giuseppe Cultrone:** Validation, Supervision, Investigation, Funding acquisition, Formal analysis, Data curation, Writing – review & editing.

Declaration of competing interest

The authors declare that they have no known competing financial interests or personal relationships that could have appeared to influence the work reported in this paper.

Data availability

Data will be made available on request.

Acknowledgements

This study has been funded by Junta de Andalucía Research Group RNM179, and the Ministry of Science and Innovation under research projects PID2020-119838RA-I00 and B-RNM-188-UGR20 of the Regional Ministry of University, Research and Innovation of the Junta de Andalucía and FEDER, *a way of making Europe*. We are grateful to Nigel Walkington for his assistance in revising the English text of the manuscript. Thanks also to the Department of Geosciences of the University of Padova.

* Funding for open access charge: Universidad de Granada / CBUA.

Appendix A. Supplementary data

Supplementary data to this article can be found online at https://doi.org/10.1016/j.susmat.2024.e00859.

References

[1] J.E. Wills, European consumption and Asian production in the seventeenth and eighteenth centuries, in: Consumption and the World of Goods, Routledge, 2013, pp. 133–147.
[2] J. Zhang, G. Ma, L. Chen, T. Liu, X. Liu, C. Lu, Profiling elements in Puerh tea from Yunnan province, China, Food Addit. Contam. Part B 10 (3) (2017) 155–164, https://doi.org/10.1080/19393210.2017.1278726.
[3] J.M.T. Hamilton-Miller, Anti-cariogenic properties of tea (Camellia sinensis), J. Med. Microbiol. 50 (4) (2001) 299–302, https://doi.org/10.1099/0022-1317-50-4-299.
[4] P. Trouillas, C.A. Calliste, D.P. Allais, A. Simon, A. Marfak, C. Delage, J.L. Duroux, Antioxidant, anti-inflammatory and antiproliferative properties of sixteen water plant extracts used in the Limousin countryside as herbal teas, Food Chem. 80 (3) (2003) 399–407, https://doi.org/10.1016/S0308-8146(02)00282-0.
[5] H. Wang, G.J. Provan, K. Helliwell, Tea flavonoids: their functions, utilisation and analysis, Trends Food Sci. Technol. 11 (4–5) (2000) 152–160, https://doi.org/10.1016/S0924-2244(00)00061-3.
[6] M.A. Farag, F. Elmetwally, R. Elghanam, N. Kamal, K. Hellal, H.S. Hamezah, A. Mediani, Metabolomics in tea products; a compile of applications for enhancing agricultural traits and quality control analysis of Camellia sinensis, Food Chem. 404 (2023) 134628, https://doi.org/10.1016/j.foodchem.2022.134628.
[7] B.E. Sumpio, A.C. Cordova, D.W. Berke-Schlessel, F. Qin, Q.H. Chen, Green tea, the "Asian paradox," and cardiovascular disease, J. Am. Coll. Surg. 202 (5) (2006) 813–825, https://doi.org/10.1016/j.jamcollsurg.2006.01.018.
[8] I. Tea Awasom, J. Agric. Food Inf. 12 (1) (2011) 12–22, https://doi.org/10.1080/10496505.2011.540552.
[9] S. Bajaj, Tea bags filter paper-a miniature textile creation, Contemp. Soc. Sci. 25 (2016) 131–138.
[10] B. Debnath, P. Duarah, M.K. Purkait, Microwave-assisted quick synthesis of microcrystalline cellulose from black tea waste (Camellia sinensis) and characterization, Int. J. Biol. Macromol. 125354 (2023), https://doi.org/10.1016/j.ijbiomac.2023.125354.
[11] S. Guo, M.K. Awasthi, Y. Wang, P. Xu, Current understanding in conversion and application of tea waste biomass: a review, Bioresour. Technol. 338 (2021) 125530, https://doi.org/10.1016/j.biortech.2021.125530.
[12] N. Tang, X. Tan, Y. Cai, M.Y. He, Z.Y. Xiang, H. Ye, J.L. Ma, Characterizations and application potentials of the hemicelluloses in waste oil-tea camellia fruit shells from southern China, Ind. Crop. Prod. 178 (2022) 114551, https://doi.org/10.1016/j.indcrop.2022.114551.

[13] Y. Feng, J. Jiang, L. Zhu, L. Yue, J. Zhang, S. Han, Effects of tea saponin on glucan conversion and bonding behaviour of cellulolytic enzymes during enzymatic hydrolysis of corncob residue with high lignin content, Biotechnol. Biofuels 6 (1) (2013) 1–8.
[14] F. Hussain, I. Hussain, A.H.A. Khan, Y.S. Muhammad, M. Iqbal, G. Soja, S. Yousaf, Combined application of biochar, compost, and bacterial consortia with Italian ryegrass enhanced phytoremediation of petroleum hydrocarbon contaminated soil, Environ. Exp. Bot. 153 (2018) 80–88, https://doi.org/10.1016/j.envexpbot.2018.05.012.
[15] M. Li, Y. Wang, Z. Shen, M. Chi, C. Lv, C. Li, X. Zhao, Investigation on the evolution of hydrothermal biochar, Chemosphere 307 (2022) 135774, https://doi.org/10.1016/j.chemosphere.2022.135774.
[16] Y. Zhang, X. Li, Y. Li, Influence of solution chemistry on heavy metals removal by bioadsorbent tea waste modified by poly (vinyl alcohol), Desalin. Water Treat. 53 (8) (2015) 2134–2143, https://doi.org/10.1080/19443994.2013.861775.
[17] U. De Corato, Agricultural waste recycling in horticultural intensive farming systems by on-farm composting and compost-based tea application improves soil quality and plant health: a review under the perspective of a circular economy, Sci. Total Environ. 738 (2020) 139840, https://doi.org/10.1016/j.scitotenv.2020.139840.
[18] L. Orden, N. Ferreiro, P. Satti, L.M. Navas-Gracia, L. Chico-Santamarta, R. A. Rodríguez, Effects of onion residue, bovine manure compost and compost tea on soils and on the agroecological production of onions, Agriculture 11 (10) (2021) 962, https://doi.org/10.3390/agriculture11100962.
[19] X. Ding, H. Li, Z. Wen, Y. Hou, G. Wang, J. Fan, L. Qian, Effects of fermented tea residue on fattening performance, meat quality, digestive performance, serum antioxidant capacity, and intestinal morphology in fatteners, Animals 10 (2) (2020) 185, https://doi.org/10.3390/ani10020185.
[20] L. Li, X. Sun, J. Luo, T. Chen, Q. Xi, Y. Zhang, J. Sun, Effects of herbal tea residue on growth performance, meat quality, muscle metabolome, and rumen microbiota characteristics in finishing steers, Front. Microbiol. 12 (2022) 821293, https://doi.org/10.3389/fmicb.2021.821293.
[21] L. Zhang, Production of bricks from waste materials–a review, Constr. Build. Mater. 47 (2013) 643–655, https://doi.org/10.1016/j.conbuildmat.2013.05.043.
[22] Z. Zhang, Y.C. Wong, A. Arulrajah, S. Horpibulsuk, A review of studies on bricks using alternative materials and approaches, Constr. Build. Mater. 188 (2018) 1101–1118, https://doi.org/10.1016/j.conbuildmat.2018.08.152.
[23] L. Crespo-López, C. Coletti, S. Morales-Ruano, G. Cultrone, Use of recycled carbon fibre as an additive in the manufacture of porous bricks more durable against salt crystallization, Ceram. Int. (2023), https://doi.org/10.1016/j.ceramint.2023.12.287.
[24] R. Ordieres, G. Cultrone, Technical quality of solid bricks made using clayey earth with added coffee grounds and fly ash, Constr. Build. Mater. 341 (2022) 127757, https://doi.org/10.1016/j.conbuildmat.2022.127757.
[25] C. Coletti, E. Bragié, M.C. Dalconi, C. Mazzoli, A. Hein, L. Maritan, A new brick-type using grape stalks waste from wine production as pore-agent, Open Ceram. 14 (2023) 100365, https://doi.org/10.1016/j.oceram.2023.100365.
[26] L. Crespo-López, A. Martínez-Ramirez, E. Sebastián, G. Cultrone, Pomace from the wine industry as an additive in the production of traditional sustainable lightweight eco-bricks, Appl. Clay Sci. 243 (2023) 107084, https://doi.org/10.1016/j.clay.2023.107084.
[27] A. Hamilton, C. Hall, The mechanics of moisture-expansion cracking in fired-clay ceramics, J. Phys. D. Appl. Phys. 46 (9) (2013) 092003, https://doi.org/10.1088/0022-3727/46/9/092003.
[28] N.S. Saman, Assessing Low Thermal Conductivity of Bricks which Contain Rice Husk, Corn Cob and Waste Tea as an Additive Material, Doctoral dissertation, Universiti Tun Hussein Onn Malaysia, 2017.
[29] S. Ozturk, M. Sutcu, E. Erdogmus, O. Gencel, Influence of tea waste concentration in the physical, mechanical and thermal properties of brick clay mixtures, Constr. Build. Mater. 217 (2019) 592–599, https://doi.org/10.1016/j.conbuildmat.2019.05.114.
[30] F. Anjum, M.Y. Naz, A. Ghaffar, S. Shukrullah, K. Kamran, A. Ghuffar, Study of microstructural, physical, thermal, and mechanical properties of organic waste–incorporated fired clay bricks in the framework of energy conservation, J. Mater. Civ. Eng. 33 (5) (2021) 04021066, https://doi.org/10.1061/(ASCE)MT.1943-5533.0003683.
[31] V. Sahu, R. Attri, P. Gupta, R. Yadav, Development of eco friendly brick using water treatment plant sludge and processed tea waste, J. Eng Design Technol. 18 (3) (2020) 727–738, https://doi.org/10.1108/JEDT-06-2019-0168.
[32] J.E.F. Ibrahim, M. Tihtih, E.İ. Şahin, M.A. Basyooni, I. Kocserha, Sustainable Zeolitic tuff incorporating tea waste fired ceramic bricks: development and investigation, Case Stud. Constr. Mater. e02238 (2023), https://doi.org/10.1016/j.cscm.2023.e02238.
[33] J. Guimerá, R. Mas, A. Alonso, Intraplate deformation in the NW Iberian chain: Mesozoic extension and tertiary contractional inversion, J. Geol. Soc. Lond. 161 (2) (2004) 291–303, https://doi.org/10.1144/0016-764903-055.
[34] G. De Vicente, R. Vegas, A. Muñoz-Martín, J.D. Van Wees, A. Casas-Sáinz, A. Sopeña, J. Fernández-Lozano, Oblique strain partitioning and transpression on an inverted rift: the Castilian branch of the Iberian chain, Tectonophysics 470 (3–4) (2009) 224–242, https://doi.org/10.1016/j.tecto.2008.11.003.
[35] L. Ezquerro, J.L. Simón, A. Luzón, C.L. Liesa, Segmentation and increasing activity in the Neogene-quaternary Teruel Basin rift (Spain) revealed by morphotectonic approach, J. Struct. Geol. 135 (2020) 104043, https://doi.org/10.1016/j.jsg.2020.104043.
[36] C. Sinusía, E.L. Pueyo, B. Azanza, A. Pocoví, Datación magnetoestratigráfica del yacimiento paleontológico de la Puebla de Valverde (Teruel), Geo-Temas 6 (4) (2004) 339–342.
[37] G. Cultrone, E. Sebastián, K. Elert, M.J. De la Torre, O. Cazalla, C. Rodriguez-Navarro, Influence of mineralogy and firing temperature on the porosity of bricks, J. Eur. Ceram. Soc. 24 (3) (2004) 547–564, https://doi.org/10.1016/S0955-2219(03)00249-8.
[38] N. Dobelin, R. Kleeberg, Profex: a graphical user interface for the Rietveld refinement program BGMN, J. Appl. Crystallogr. 48 (2015) 1573–1580, https://doi.org/10.1107/S1600576715014685.
[39] J. Kim, E. Heo, S.J. Kim, J.Y. Kim, Investigation of the mineral components of porcelain raw material and their phase evolution during a firing process by using a Rietveld quantitative analysis, J. Korean Phys. Soc. 68 (2016) 126–130, https://doi.org/10.3938/jkps.68.126.
[40] X. Zhou, D. Liu, H. Bu, L. Deng, H. Liu, P. Yuan, H. Song, XRD-based quantitative analysis of clay minerals using reference intensity ratios, mineral intensity factors, Rietveld, and full pattern summation methods: a critical review, Solid Earth Sci. 3 (1) (2018) 16–29, https://doi.org/10.1016/j.sesci.2017.12.002.
[41] G. Christidis, K. Paipoutlidi, I. Marantos, V. Perdikatsis, Determination of amorphous matter in industrial minerals with X-ray diffraction using Rietveld refinement, Bull. Geol. Soc. Greece 56 (1) (2020) 1–16, https://doi.org/10.12681/bgsg.20940.
[42] ISO, EN 12571, Hygrothermal Performance of Building Materials and Products-Determination of Hygroscopic Sorption Properties, CEN, Belgium, 2000, p. 1997.
[43] UNE-EN, 13755. Métodos de ensayo para piedra natural: Determinación de la absorción de agua a presión atmosférica, AENOR. Madrid. (2008).
[44] NORMAL 19/88, Misura dell'indice di Asciugamento (Drying Index), CNR-ICR, Roma, Italia, 1988.
[45] UNE-EN 1926, Métodos de ensayo para piedra natural. Determinación del coeficiente de absorción de agua por capilaridad, AENOR, Madrid, 2007.
[46] UNE-EN 1936, Métodos de ensayo para piedra natural. Determinación de la densidad real y aparente y de la porosidad abierta y total, AENOR, Madrid, 2007.
[47] C. Coletti, G. Cultrone, L. Maritan, C. Mazzoli, Combined multi-analytical approach for study of pore system in bricks: how much porosity is there? Mater. Charact. 121 (2016) 82–92, https://doi.org/10.1016/j.matchar.2016.09.024.
[48] S. Salvini, C. Coletti, L. Maritan, M. Massironi, M. Balsamo, C. Mazzoli, Exploring the pore system of carbonate rocks through a multi- analytical approach, Environ. Earth Sci. Inpress. (2023), https://doi.org/10.21203/rs.3.rs-3289391/v1.
[49] C.A. Schneider, W.S. Rasband, K.W. Eliceiri, NIH image to ImageJ: 25 years of image analysis, Nat. Methods 9 (7) (2012) 671–675, https://doi.org/10.1038/nmeth.2089.
[50] E. Bwayo, S.K. Obwoya, Coefficient of Thermal Diffusivity of Insulation Brick Developed from Sawdust and Clays, Journal of Ceramics 2014, Hindawi Publishing Corporation, 2014, https://doi.org/10.1155/2014/861726. Article ID 861726, 6 pages.
[51] M. Kubiś, K. Pietrak, Ł. Cieślikiewicz, P. Furmański, M. Wasik, M. Seredyński, T. S. Wiśniewski, P. Łapka, On the anisotropy of thermal conductivity in ceramic bricks, J. Build. Eng. 31 (2020) 101418, https://doi.org/10.1016/j.jobe.2020.101418.
[52] UNE-EN 196-1, Métodos de ensayo de cementos. Parte 1: Determinación de resistencias mecánicas, AENOR, Madrid, 2005.
[53] UNE-EN 15886, Métodos de ensayo. Medición del color de superficies, AENOR, Madrid, 2011.
[54] UNE-EN 12370, Métodos de ensayo para piedra natural. Determinación de la resistencia a la cristalización de sales, AENOR, Madrid, 2002.
[55] C. Martínez-García, D. Eliche-Quesada, L. Pérez-Villarejo, F.J. Iglesias-Godino, F. A. Corpas-Iglesias, Sludge valorization from wastewater treatment plant to its application on the ceramic industry, J. Environ. Manag. 95 (2012) S343–S348, https://doi.org/10.1016/j.jenvman.2011.06.016.
[56] E. Ceramic Gliozzo, technology., How to reconstruct the firing process, Archaeol. Anthropol. Sci. 12 (11) (2020) 260, https://doi.org/10.1007/s12520-020-01133-y.
[57] Y. Maniatis, M.S. Tite, Technological examination of Neolithic-bronze age pottery form central and Southeast Europe and from the near east, J. Archaeol. Sci. 8 (1981) 59–76, https://doi.org/10.1016/0305-4403(81)90012-1.
[58] L. Crespo-López, G. Cultrone, Improvement in the petrophysical properties of solid bricks by adding household glass waste, J. Build. Eng. 59 (2022) 105039, https://doi.org/10.1016/j.jobe.2022.105039.
[59] W.L. Brown, I. Parsons, Alkali feldspars: ordering rates, phase transformations and behaviour diagrams for igneous rocks, Mineral. Mag. 53 (369) (1989) 25–42, https://doi.org/10.1180/minmag.1989.053.369.03.
[60] G. Cultrone, F.J.C. Rosua, Growth of metastable phases during brick firing: mineralogical and microtextural changes induced by the composition of the raw material and the presence of additives, Appl. Clay Sci. 185 (2020) 105419, https://doi.org/10.1016/j.clay.2019.105419.
[61] L. Nodari, E. Marcuz, L. Maritan, C. Mazzoli, U. Russo, Hematite nucleation and growth in the firing of carbonate-rich clay for pottery production, J. Eur. Ceram. Soc. 27 (16) (2007) 4665–4673, https://doi.org/10.1016/j.jeurceramsoc.2007.03.031.
[62] V. Trincal, V. Benavent, H. Lahalle, B. Balsamo, G. Samson, C. Patapy, M. Cyr, Effect of drying temperature on the properties of alkali-activated binders-recommendations for sample preconditioning, Cem. Concr. Res. 151 (2022) 106617, https://doi.org/10.1016/j.cemconres.2021.106617.
[63] M. Daghmehchi, C. Coletti, D.H. Moon, M.E.E. Jelodar, H. Omrani, A.A. Reka, M. Emami, Mineralogical and microstructural characterization of ceramics from the fifth and fourth millennium BC in the central plateau of Iran, Open Ceram. 15 (2023) 100427, https://doi.org/10.1016/j.oceram.2023.100427.

[64] L.N. Warr, Recommended abbreviations for the names of clay minerals and associated phases, Clay Miner. 55 (3) (2020) 261–264, https://doi.org/10.1180/clm.2020.30.
[65] G. Cultrone, C. Rodriguez-Navarro, E. Sebastian, O. Cazalla, M.J. De La Torre, Carbonate and silicate phase reactions during ceramic firing, Eur. J. Mineral. 13 (3) (2001) 621–634, https://doi.org/10.1127/0935-1221/2001/0013-0621.
[66] L.G. Love, Mircro-organisms and the presence of syngenetic pyrite. Quarterly, J. Geol. Soc. Lond. 113 (1–4) (1957) 429–440, https://doi.org/10.1144/GSL.JGS.1957.113.01-04.18.
[67] R.A. Berner, The synthesis of framboidal pyrite, Econ. Geol. 64 (4) (1969) 383–384.
[68] Z. Sawlowicz, Pyrite framboids and their development: a new conceptual mechanism, Geol. Rundsch. 82 (1993) 148–156, https://doi.org/10.1007/BF00563277.
[69] C. Germinario, G. Cultrone, L. Cavassa, A. De Bonis, F. Izzo, A. Langella, C. Grifa, Local production and imitations of late Roman pottery from a well in the Roman necropolis of Cuma in Naples, Italy, Geoarchaeology 34 (1) (2019) 62–79, https://doi.org/10.1002/gea.21703.
[70] W.E. Brownell, W.E. Brownell, Mineralogical composition of structural clay products, Struct. Clay Prod. 24-42 (1976), https://doi.org/10.1007/978-3-7091-8449-3_2.
[71] J. Dacuba, E. Cifrian, M. Romero, T. Llano, A. Andrés, Influence of unburned carbon on environmental-technical behaviour of coal fly ash fired clay bricks, Appl. Sci. 12 (8) (2022) 3765, https://doi.org/10.3390/app12083765.
[72] L. Crespo-López, D. Benavente, S. Morales-Ruano, M. Vázquez-Vílchez, G. Cultrone, Non-destructive techniques (NDT) and statistical analysis for the characterization of bricks made with added glass, Constr. Build. Mater. 408 (2023) 133583, https://doi.org/10.1016/j.conbuildmat.2023.133583.
[73] C. Coletti, L. Maritan, G. Cultrone, A. Hein, M.C. Dalconi, E. Molina, C. Mazzoli, Recycling trachyte waste from quarry to brick industry: effects on petrophysical properties and durability of new bricks, Constr. Build. Mater. 166 (2018) 792–807, https://doi.org/10.1016/j.conbuildmat.2018.01.158.
[74] M. Suctu, Influence of expanded vermiculite on physical properties and thermal conductivity of clay bricks, Ceram. Int. 41 (2015) 2819–2827, https://doi.org/10.1016/j.ceramint.2014.10.102.
[75] J.G. Ten, M.J. Orts, A. Saburit, G. Silva, Thermal conductivity of traditional ceramics. Part I: influence of bulk density and firing temperature, Ceram. Int. 36 (6) (2010) 1951–1959, https://doi.org/10.1016/j.ceramint.2010.05.012.
[76] I. Allegretta, G. Eramo, D. Pinto, A. Hein, The effect of mineralogy, microstructure and firing temperature on the effective thermal conductivity of traditional hot processing ceramics, Appl. Clay Sci. 135 (2017) 260–270, https://doi.org/10.1016/j.clay.2016.10.001.
[77] P. Saravanapavan, L.L. Hench, Mesoporous calcium silicate glasses. I. Synthesis, J. Non-Cryst. Solids 318 (1–2) (2003) 1–13, https://doi.org/10.1016/S0022-3093(02)01864-1.
[78] M. Dondi, G. Guarini, M. Raimondo, C. Zanelli, Recycling PC and TV waste glass in clay bricks and roof tiles.J, Waste Manag. 29 (6) (2009) 1945–1951, https://doi.org/10.1016/j.wasman.2008.12.003.
[79] Pliego RL-88, Pliego General de Condiciones para la Recepción de Ladrillos Cerámicos en las Obras de Construcción, Ministerio de Obras Públicas, Transportes y Medio Ambiente, 1988. Spain.
[80] O. Molina, V. Vilarrasa, M. Zeidouni, Geologic carbon storage for shale gas recovery, Energy Procedia 114 (2017) 5748–5760, https://doi.org/10.1016/j.egypro.2017.03.1713.
[81] S. Kumar Thota, T. Duc Cao, F. Vahedifard, Poisson's ratio characteristic curve of unsaturated soils, J. Geotech. Geoenviron. Eng. 147 (1) (2021), https://doi.org/10.1061/(ASCE)GT.1943-5606.0002424, 04020149.
[82] E.M. Pérez-Monserrat, L. Maritan, G. Cultrone, Firing and post-firing dynamics of Mg-and Ca-rich bricks used in the built heritage of the city of Padua (northeastern Italy), European Journal of Mineralogy 34 (3) (2022) 301–319, https://doi.org/10.5194/ejm-34-301-2022.
[83] E.M. Pérez-Monserrat, L. Crespo-López, G. Cultrone, P. Mozzi, L. Maritan, Clayey materials for traditional bricks production in North-Eastern Italy through a combined compositional study: From firing dynamics to provenance, Journal of Archaeological Science: Reports 54 (2024) 104400, https://doi.org/10.1016/j.jasrep.2024.104400.